

- (24) Kirkwood, J. G. *J. Polym. Sci.* **1954**, *12*, 1.
- (25) Ouano, A. C.; Johnson, D. E.; Dawson, B.; Pederson, L. A. *J. Polym. Sci., Polym. Chem. Ed.* **1976**, *14*, 701.
- (26) Ouano, A. C. In *Polymers in Electronics*; Davidson, T., Ed.; ACS Symposium Series 242; American Chemical Society: Washington, DC, 1984, pp 79-90.
- (27) Cooper, W. J.; Krasicky, P. D.; Rodriguez, F. *J. Appl. Polym. Sci.* **1986**, *31*, 65.
- (28) Levinson, M.; Wilkins, C. W., Jr. *J. Electrochem. Soc.* **1986**, *133*, 619.
- (29) Timmermans, J. *Physicochemical Constants of Pure Organic Compounds*; Elsevier: New York, 1965; Vol. II.
- (30) Norisuye, T.; Fujita, H. *Polym. J. (Tokyo)* **1982**, *14*, 143.
- (31) Vacatello, M.; Flory, P. J. *Macromolecules* **1986**, *19*, 405.
- (32) Sundararajan, P. R. *Macromolecules* **1986**, *19*, 415.
- (33) Yoon, D. Y.; Sundararajan, P. R.; Flory, P. J. *Macromolecules* **1975**, *8*, 776.
- (34) Wang, F. W. *J. Polym. Sci., Polym. Phys. Ed.* **1975**, *13*, 1215.
- (35) Zimm, B. H. *Macromolecules* **1984**, *17*, 795.
- (36) Tricot, M. *Macromolecules* **1986**, *19*, 1268.
- (37) de la Torre, J. G.; Martinez, M. C. L.; Tirado, M. M.; Freire, J. J. *Macromolecules* **1984**, *17*, 2715.
- (38) Section 5, Chapter 1 of ref 1.
- (39) Appendix G of ref 1.

## Excluded-Volume Effects on Force-Length Relations of Long-Chain Molecules<sup>1</sup>

J. Gao and J. H. Weiner\*

Department of Physics and Division of Engineering, Brown University, Providence, Rhode Island 02912. Received June 30, 1986

**ABSTRACT:** The force-length relation  $f(r)$  for a freely jointed chain with excluded volume has been determined by Monte Carlo techniques for chains with up to  $N = 200$  bonds for the strain ensemble ( $r$  fixed and  $f$  fluctuates). As in the recent treatment for chains with  $N = 10$  bonds, it is found that excluded-volume effects in this ensemble cause  $f$  to be compressive ( $f < 0$ ) for small  $r$ , in contrast to the stress ensemble ( $f$  fixed and  $r$  fluctuates) that leads to  $f \geq 0$  for all  $r$ . However, in contrast to the results for short chains, the force-length relation for longer chains varies smoothly and monotonically and shows all of the generally observed characteristics of experiments on rubber-like materials in uniaxial tension. The results are interpreted in terms of a statistical mechanics framework that computes, as a function of  $r$ , the fraction of the configuration space region that is accessible to the phantom chain, which becomes inaccessible due to excluded volume. It is found that this fraction, which is zero for the fully extended chain, becomes large quite rapidly as  $r$  decreases. The force-length relation for pairs of interacting chains with common end-to-end displacement vector  $\mathbf{r}$  is also computed by a Monte Carlo technique. Chain-chain interaction is found to have little effect. Molecular dynamics calculations determine the separate contributions of the covalent and noncovalent potentials to the force and provide insight into the nature of the transmission of forces in the molecule.

### I. Introduction

This paper continues and extends earlier work<sup>2,3</sup> on excluded-volume effects on the force-displacement relation,  $f(r)$ , for a long-chain molecule whose atoms are in thermal motion with large amplitude consistent with the constraints imposed by the covalent bonds between neighboring atoms. In the notation we employ,  $\mathbf{r}$  is the displacement between the end atoms of the chain;  $\mathbf{f}$  and  $-\mathbf{f}$  are the forces applied to these end atoms; and  $r = |\mathbf{r}|$ ,  $f = \mathbf{f} \cdot \mathbf{r} / r$ . By the convention adopted,  $f > 0$  corresponds to a tensile force, while  $f < 0$  corresponds to a compressive force.

Although it also finds application to aspects of polymer solution and melt behavior, the importance of this relation lies mainly in the subject of rubber elasticity, which treats amorphous, cross-linked networks of such chains. In this context, we may think of the forces  $\mathbf{f}$  and  $-\mathbf{f}$  as applied to the chain through the cross-linking junctions. The mechanical behavior of such networks for different types of non-Gaussian models of polymer molecules is often studied on the basis of the three-chain model of rubber elasticity,<sup>4</sup> which makes direct application of the force-length relation.

From the viewpoint of equilibrium statistical mechanics, we can distinguish between two types of ensembles for the calculation of the force-displacement relation  $f(r)$ . In the first, the end atoms are fixed with displacement  $\mathbf{r}$  between them, and the force  $\mathbf{f}$  that must be applied to the end atoms fluctuates as the free atoms of the chain undergo thermal motion. We refer to this as a strain ensemble<sup>5</sup> in analogy to the term volume ensemble for a gas. For this

case, the phase-average  $\langle f \rangle = \langle \mathbf{f} \rangle \cdot \mathbf{r} / r$  is identified with  $f$  to obtain the  $f(r)$  relation.

In the second statistical ensemble, one end of the chain is fixed at the origin, a fixed force  $\mathbf{f}$  is applied to the other end, and the displacement  $\mathbf{r}$  fluctuates. We refer to this as a stress ensemble,<sup>5</sup> in analogy to the term pressure ensemble for a gas. For this case, the phase-average  $\langle r_f \rangle = \langle \mathbf{r} \rangle \cdot \mathbf{f} / |\mathbf{f}|$  is identified with  $r$  to obtain the  $f(r)$  relation.

For a gas it is generally assumed and can be rigorously demonstrated for reasonable mathematical models<sup>6</sup> that the pressure and volume ensembles are equivalent in the macroscopic limit. This does not appear to be the case for the corresponding stress and strain ensembles for a single polymer chain.<sup>3,7,8</sup> Although both the stress and strain ensembles predict purely tensile relations ( $f > 0$  for all  $r$ ), if excluded volume effects are ignored, the situation is changed when the latter are treated in the model. In that case, the stress (constant  $\mathbf{f}$ ) ensemble still leads to a purely tensile relation, but the strain (constant  $\mathbf{r}$ ) ensemble yields  $f < 0$  for sufficiently small  $r$ .

A further distinction between the  $p(v, T)$  relation for a gas and the  $f(r, T)$  relation for a long-chain molecule may be made in terms of fluctuations. For the gas,  $\Delta p / p$ , the relative fluctuations in pressure in the volume ensemble become vanishingly small for sufficiently large systems. For the polymer molecule, on the other hand,  $\Delta f / f$ , the relative fluctuations in the force in the strain ensemble, remain large, regardless of the length of the chain.<sup>9</sup>

The previous work of Berman and Weiner<sup>3</sup> on excluded-volume effects on the force-length relation relied on

molecular dynamics and was restricted to chains with only  $N = 10$  bonds. In this work, Monte Carlo procedures are used to study chains with up to  $N = 200$  bonds. Further aspects of this problem are also treated in this paper: (a) The effect of chain-chain interaction is studied for pairs of interacting chains. (b) A theoretical framework is developed that permits the calculation of the fraction of configuration space that becomes inaccessible due to excluded-volume interactions for different degrees of chain extension. (c) The Monte Carlo calculations are supplemented by molecular dynamics in order to gain insight into the nature of force transmission in the chain by noncovalent interactions.

The plan of the paper is as follows: The Monte Carlo results for long single chains are presented in section II. The theory for calculating the fraction of configuration space rendered inaccessible by excluded-volume interactions is developed in section III and applied to the numerical results of the previous section. We then use molecular dynamics techniques in section IV to calculate appropriate force decompositions. Monte Carlo methods are used in section V to study the effect of chain-chain interaction. Conclusions that may be drawn from this work and their implications for the theory of rubber elasticity are presented in section VI. An appendix contains details of the Monte Carlo procedures employed.

## II. Monte Carlo Results for Single Chains

We treat a freely jointed chain with  $N$  bonds of length  $a$ . Atom positions are denoted by  $\mathbf{x}_i$ ,  $i = 0, 1, \dots, N$ ; atoms 0 and  $N$  are fixed in position with  $\mathbf{x}_N - \mathbf{x}_0 = \mathbf{r}$ , and atoms 1 through  $N - 1$  are free to execute thermal motion. The covalent bonds between neighboring atoms along the chain are represented by stiff linear springs with potential

$$V_C = \frac{1}{2}k[|\mathbf{x}_i - \mathbf{x}_{i-1}| - a]^2, \quad i = 1, \dots, N \quad (1)$$

where  $a$  is the equilibrium bond length. The excluded-volume repulsive force, or noncovalent interaction, is represented by the hard-sphere potential

$$V_E(\mathbf{x}_0, \dots, \mathbf{x}_N) = \begin{cases} 0 & \text{for } |\mathbf{x}_r - \mathbf{x}_s| > \sigma, \text{ all } r \neq s \\ \infty & \text{for } |\mathbf{x}_r - \mathbf{x}_s| < \sigma, \text{ some } r \neq s \end{cases} \quad (2)$$

The use of stiff linear springs to represent the covalent bonds means that we are employing what has been termed a flexible model<sup>5,10-12</sup> for the chain. In the large- $\kappa$  limit, it may then be shown<sup>13</sup> that the strain-ensemble force-length relation  $f(r, T)$  may be computed from

$$f = -kT \frac{\partial}{\partial r} \log p \quad (3)$$

where  $p(\mathbf{r})$  is the probability density for a displacement  $\mathbf{r}$  in a random walk of step size  $a$  subject to the excluded-volume restriction.

Details of the Monte Carlo procedure employed are given in the Appendix. It yields numerical estimates of  $P(r)\Delta r$ , the fraction of time spent with  $r$  in the interval  $r$  to  $r + \Delta r$ . The values of  $p(\mathbf{r})$  are then determined by use of the relation  $P(r) = 4\pi r^2 p(\mathbf{r})$ , and the force  $f$  follows from eq 3 by suitable numerical differentiation techniques.<sup>14</sup> Typical examples of the force-length relation obtained in this way are shown in Figure 1, in which the points represent the values obtained from the numerical differentiation and, for the case of  $\sigma/a = 0.8$ , the curve is a cubic spline fit through these points. As a check of the numerical procedure, it is applied also to the case with no excluded volume,  $\sigma = 0$ . These numerical results are compared in Figure 1 with the known theoretical solution.

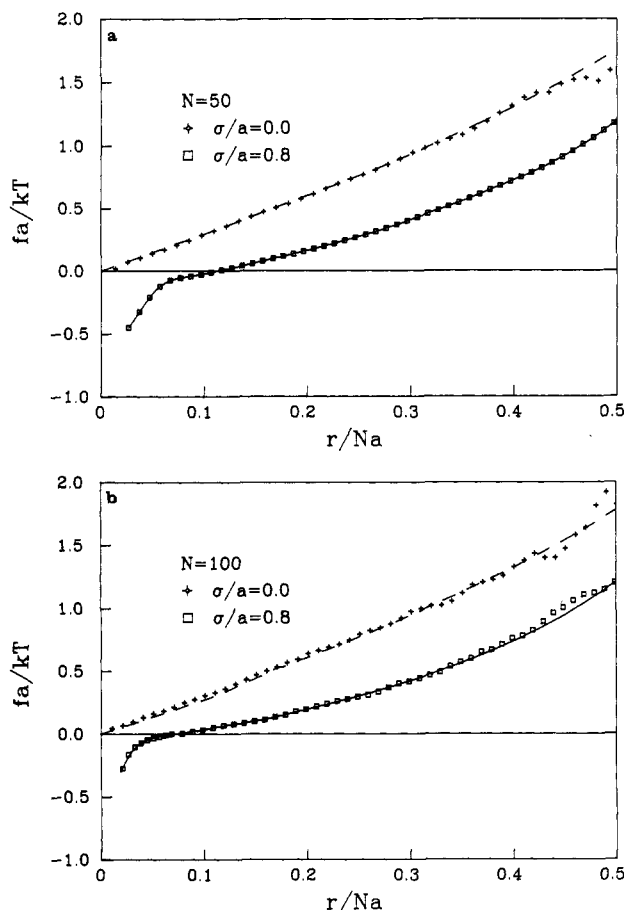


Figure 1. Force-length relation for freely jointed chain with (a)  $N = 50$  bonds and (b)  $N = 100$  bonds. Points result from numerical differentiation of probability distribution obtained by Monte Carlo procedure. Dashed curve is theoretical result for  $\sigma/a = 0$ . Solid curve is cubic spline fit through the points for  $\sigma/a = 0.8$ .

As with the earlier results<sup>3</sup> obtained for  $N = 10$ , the results for  $N = 50$  and  $N = 100$  show the existence of an  $r_0$  with  $f$  compressive for  $r < r_0$  and  $f$  tensile for  $r > r_0$ . However, the relation for  $N = 10$  showed considerable structure, including nonmonotonic behavior for  $r < r_0$ , whereas the relation for  $N = 50$  is smooth and monotonic and has, in fact, the general character of the observed stress-strain behavior for rubber in uniaxial deformation.

The probability distribution  $P(r)$  determined by the Monte Carlo procedure was also used to determine  $\langle r^2 \rangle_0^{1/2}$ , the root-mean-square end-to-end distance for zero applied force in a stress ensemble. On the basis of computations for  $N$  from 10 to 200, it is found, to good approximation, that  $\langle r^2 \rangle_0^{1/2} = CN^\nu$ , with  $\nu = 0.61$ .

Oono, Ohta, and Freed<sup>15</sup> have used renormalization group techniques to obtain the  $p(\mathbf{r})$  relation for a polymer chain with excluded volume in the form

$$p(\mathbf{r}) = 0.33\rho^{0.25} \exp(-1.5\rho^{2.25} + 0.1\rho^2) \quad (4)$$

where

$$\rho = r/\langle r^2 \rangle_0^{1/2}$$

In Figure 2 we compare the force-length relation based on this expression for  $p(r)$ , using eq 3 and the value of  $\langle r^2 \rangle_0^{1/2}$  found in the Monte Carlo calculations, with the force-length relations based on the Monte Carlo probability distribution. It is seen that the two results are in reasonably good agreement at small to moderate values of  $r/Na$ , with the agreement better for  $N = 100$  than for  $N = 50$ , although the renormalization group result, as is

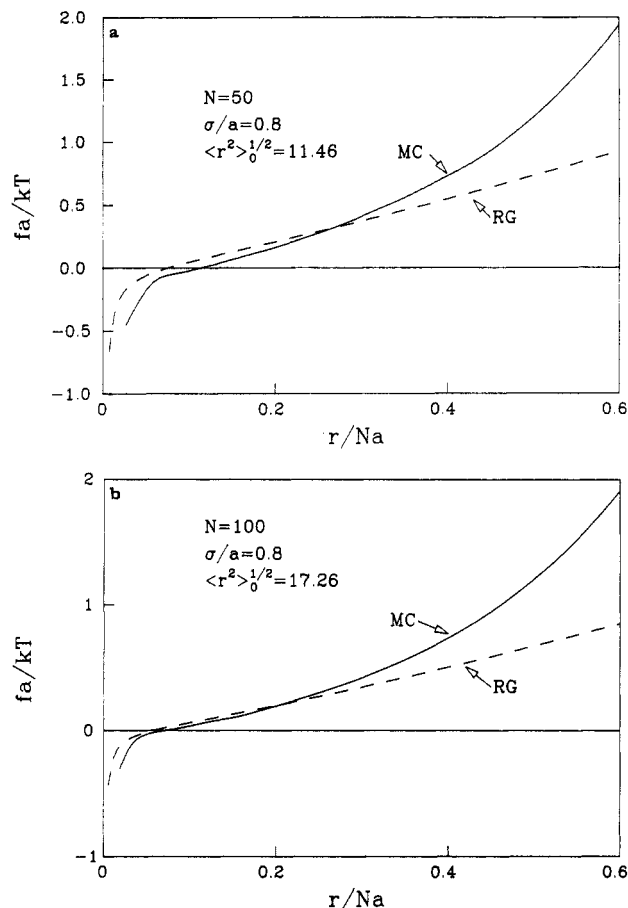


**Figure 2.** Force-length relations as obtained by Monte Carlo procedure (MC) and by renormalization group calculations (RG) of Oono et al.<sup>15</sup> (a)  $N = 50$ ; (b)  $N = 100$ .

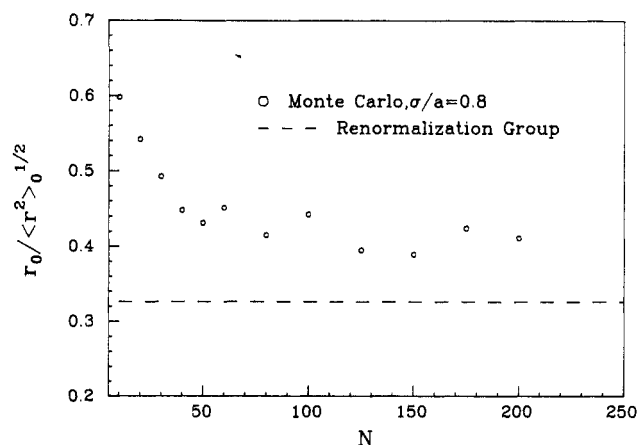


**Figure 3.** Comparison of values of  $r_0/\langle r^2 \rangle_0^{1/2}$  as determined by the Monte Carlo calculations with the ratio  $r_0/\langle r^2 \rangle_0^{1/2} = 0.326$  predicted by the renormalization group calculations of Oono et al.<sup>15</sup>

to be expected, does not show the upturn in the force at large values of  $r/Na$  found in the numerical results.

It is seen from eq 3 and 4 that the renormalization group result predicts a value of  $r_0$ , the end-to-end spacing at which  $f = 0$  in a strain ensemble, given by the relation  $r_0 = 0.326\langle r^2 \rangle_0^{1/2}$ . In Figure 3, we compare the values of  $r_0/\langle r^2 \rangle_0^{1/2}$  as determined by the Monte Carlo calculations for various values of  $N$  with the renormalization group result. Although the values of this ratio obtained by Monte Carlo appear to be approaching a constant value as  $N$  increases, the computed limit appears to be somewhat larger than the theoretical value. However, it should be

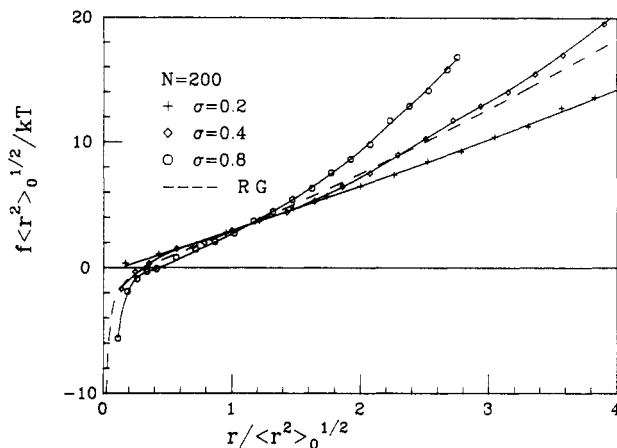


**Figure 4.** Force-length relations as determined by computer simulation for different hard-sphere diameters  $\sigma$  compared with renormalization group calculations (RG) of Oono et al.<sup>15</sup>

noted that it is difficult to find the value of  $r_0$  accurately, and therefore further calculations will be necessary to resolve this point.

The numerical results thus far described have all been for a hard-sphere diameter  $\sigma = 0.8a$ . The effect of variation of  $\sigma$  on the force-length relation is shown in Figure 4 where they are compared with the renormalization group results of Oono et al.<sup>15</sup> It is seen that for the fixed value of  $N = 200$ , the Monte Carlo result for  $\sigma = 0.4a$  agrees best with the renormalization group result, whereas there is substantial deviation for  $\sigma = 0.2a$  and  $\sigma = 0.8a$ . In particular, the Monte Carlo results for  $\sigma = 0.2a$  do not show a compressive regime for the range of  $R$  for which numerical data are available. Whether these differences would persist for larger  $N$  or whether they indicate a  $\sigma$ -dependent rate of convergence<sup>16</sup> to the renormalization group results remains a subject for future study. It is also of interest to note that the various curves in Figure 4 appear to have a common crossing point at  $r/\langle r^2 \rangle_0^{1/2} \approx 1.2$ .

### III. Excluded Volume in Configuration Space

The partition function  $Z(\mathbf{r}, T)$  for the strain ensemble of the flexible model described in the previous section is

$$Z(\mathbf{r}, T) = C \int_{\Gamma_{\text{conf}}} e^{-\beta V} d\mathbf{x}_1 \dots d\mathbf{x}_{N-1} \quad (5)$$

where  $V = V_C + V_E$  with the covalent potential  $V_C$  defined in eq 1 and the excluded-volume potential  $V_E$  defined in eq 2. Here, in eq 5, and in what follows,  $C$  denotes a quantity independent of  $\mathbf{r}$ .

In order to evaluate the asymptotic approximation of  $Z(\mathbf{r}, T)$  valid for arbitrarily large  $\kappa$ , it is convenient to introduce an appropriate curvilinear coordinate system  $q^1, \dots, q^n$ , where  $n = 3(N-1)$ , through the transformation

$$\mathbf{x}_j = \mathbf{x}_j(q^1, \dots, q^n; \mathbf{r}), \quad j = 1, \dots, N-1 \quad (6)$$

such that  $q^\alpha$ ,  $\alpha = 1, \dots, f$ , correspond to easy motion (i.e., to small changes in  $V_C$ ) even for large  $\kappa$ , while  $q^A$ ,  $A = f+1, \dots, n$ , can only assume values in the neighborhood of zero when  $\kappa$  is large. It may then be shown<sup>5</sup> that the asymptotic, large  $\kappa$ , approximation to  $Z$  takes the form

$$Z(\mathbf{r}, T) = C \int_{\Gamma_{q^A}} e^{-\beta V_E} |g_{ij}|_0^{1/2} dq^1 \dots dq^f \quad (7)$$

where the integration is now confined to the  $f$ -dimensional configuration space  $\Gamma_{q^A}$  of the "soft" variables  $q^A$ . The quantity  $g_{ij}$ ,  $i, j = 1, \dots, n$ , is the metric tensor of the coordinate transformation of eq 6, and  $|g_{ij}|_0$  is the determinant of this tensor with  $q^A = 0$ ,  $A = f+1, \dots, n$ . Note that in the large- $\kappa$  approximation, both  $|g_{ij}|_0$  and  $V_E$  are

functions of  $q^1, \dots, q^f$  and  $\mathbf{r}$ . We next write

$$Z(\mathbf{r}, T) = C(D(\mathbf{r}) - E(\mathbf{r})) \quad (8)$$

where

$$D(\mathbf{r}) = \int_{\Gamma_{q^\alpha}} |g_{ij}|_0^{1/2} dq^1 \dots dq^f \quad (9)$$

and

$$E(\mathbf{r}) = \int_{\Gamma_{q^\alpha}} (1 - e^{-\beta V_E}) |g_{ij}|_0^{1/2} dq^1 \dots dq^f \quad (10)$$

The quantity  $D(\mathbf{r})$  may be given the following geometrical interpretation.<sup>17</sup> Since the soft variables  $q^\alpha$  correspond to angle variables, we may speak of the configurational space  $\Gamma_{q^\alpha}$  as a piece of an  $f$ -dimensional torus and, as the chain is stretched, the system is confined to an increasingly smaller portion of this torus.  $D(\mathbf{r})$  may be visualized as the  $n$ -dimensional volume of a shell whose inner surface is  $\Gamma_{q^\alpha}$ . The "thickness" of the shell is an  $(n - f)$ -dimensional volume that varies with  $q^\alpha$ , this variation being a reflection, in the large- $\kappa$  asymptotic approximation, of the variable amplitude of the thermal vibrations that the flexible constraints permit in the  $q^A$  directions. For brevity in what follows we will refer to  $D(\mathbf{r})$  as the phantom volume; it is the volume in configuration space to which the equivalent phantom chain<sup>18</sup> (excluded-volume interactions ignored) is confined for a given displacement  $\mathbf{r}$ .

Since the quantity  $1 - e^{-\beta V_E} = 1$  only when two atoms overlap and is zero otherwise, it is clear that  $E(\mathbf{r})$  is that portion of the phantom volume  $D(\mathbf{r})$  that becomes inaccessible to the system due to excluded-volume interactions; we will refer to  $E(\mathbf{r})$  as the excluded volume and to  $D - E$  as the available volume.

For the strain ensemble, the force is obtained from the partition function  $Z(\mathbf{r}, T)$  by the relation

$$f = -kT \frac{\partial}{\partial r} \log Z(\mathbf{r}, T) \quad (11)$$

It then follows from eq 8 that

$$f = \frac{-kT}{D - E} \left( \frac{\partial D}{\partial r} - \frac{\partial E}{\partial r} \right) \quad (12)$$

In the absence of excluded volume ( $E \equiv 0$ ) this relation becomes

$$f_{ph} = -\frac{kT}{D} \frac{dD}{dr} \quad (13)$$

where  $f_{ph}$  denotes the force in a chain without excluded volume, i.e., a phantom chain. Equations 12 and 13 may be recast, by straightforward manipulations, in the form

$$\frac{d}{dr} \left( \frac{E}{D} \right) = \frac{1}{kT} \left( \frac{E}{D} - 1 \right) \Delta \quad (14)$$

where

$$\Delta(r) = f_{ph}(r) - f(r) \quad (15)$$

It is readily verified that  $E/D = 0$  at  $r = Na$ , i.e., for the fully extended chain. Since  $f_{ph}(r)$  is known analytically and  $f(r)$  has been determined numerically in the previous section, we may integrate eq 15 numerically subject to this boundary condition at  $r = Na$ . The required values of  $\Delta(r)$  are obtained from curves such as those shown in Figure 5. Examples of these solutions are shown in Figure 6. These results show that  $E/D$  becomes surprisingly large even at such relatively large extensions as  $r/Na \approx 0.4$  and, as might be expected,  $E/D$  decreases with decreasing  $\sigma$ .

#### IV. Molecular Dynamics Results

In order to gain further insight into the excluded-volume effects on the force-length relation for chains in the strain

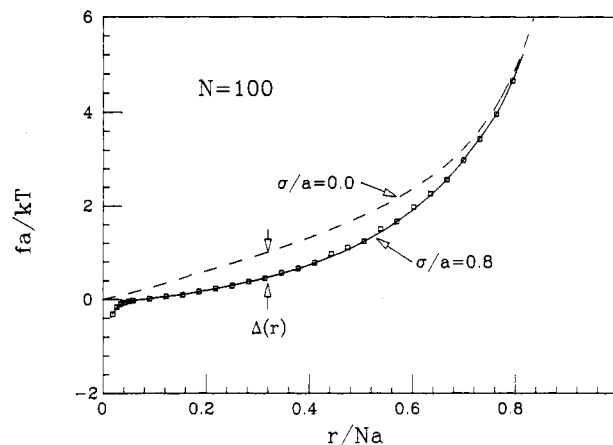


Figure 5. Full force-length relation curve showing the difference,  $\Delta(r)$ , between phantom chain ( $\sigma = 0$ ) and chain with excluded volume ( $\sigma/a = 0.8$ ).

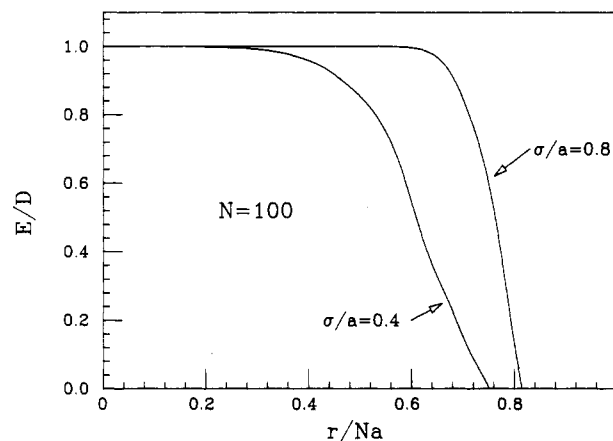


Figure 6. Fraction,  $E/D$ , of volume  $D$  in configuration space accessible to a phantom chain which is prohibited by excluded volume. Hard-sphere diameter  $\sigma = 0.4a$  and  $0.8a$ .

ensemble, the Monte Carlo calculations described in section II were supplemented by molecular dynamics simulations. The model used was again a freely jointed chain with the covalent bonds represented by  $V_C$  of eq 1; the excluded-volume repulsive force, or noncovalent interaction, is represented by a truncated Lennard-Jones potential

$$V_{NC}(s) = 4\epsilon[(\sigma/s)^{12} - (\sigma/s)^6] \quad \text{for } s \leq s_0 \\ = V_{NC}(s_0) \quad \text{for } s \geq s_0 \quad (16)$$

where  $s$  is the distance between any pair of atoms and  $s_0 = 2.25\sigma$ .

While the Monte Carlo calculations were for the case of asymptotically large spring constant  $\kappa$ , in this section a value of  $\kappa$  somewhat softer than that of a carbon backbone chain was used in order to facilitate the calculations; namely,  $\kappa$  corresponds to  $\omega_0 = (\kappa/m)^{1/2} = 4.1 \times 10^{13} \text{ s}^{-1}$ . The temperature  $T = 300 \text{ K}$  and  $kT/\epsilon = 20$ , where  $\epsilon$  is the parameter in eq 16. The time step  $\Delta t = 2.4 \times 10^{-15} \text{ s}$  was used.

As part of these calculations, the relative contributions of the covalent and noncovalent potentials to the forces in the molecule were determined. A typical example is shown in Figure 7, in which is plotted  $f_i$ , the time average of the resultant force in the  $\mathbf{r}$  direction exerted by atoms  $i + 1, \dots, N$  upon the atoms  $0, \dots, i$ ;  $f_i^C$  is the covalent portion of this force due to  $V_C$ , and  $f_i^{NC}$  is the noncovalent portion due to  $V_{NC}$ , so that  $f_i = f_i^C + f_i^{NC}$ . Both  $f_i^C$  and  $f_i^{NC}$  show some end-effect variation near the ends of the chain but are relatively constant over the central portion of the chain.

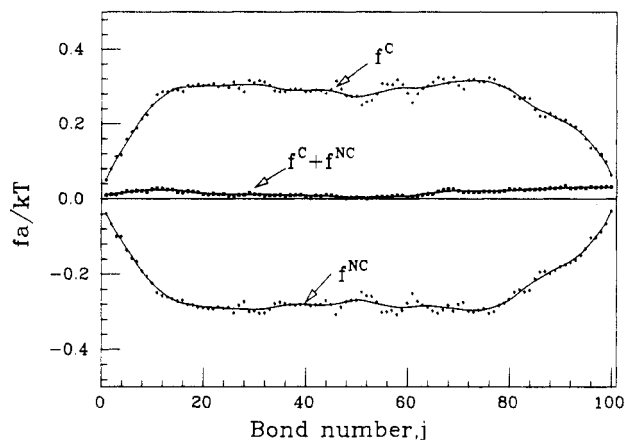


**Figure 7.** Force decomposition into covalent component,  $f^C$ , and noncovalent component,  $f^{NC}$ , obtained by molecular dynamics in strain ensemble. The total bond number  $N = 100$ , and  $r/Na = 0.1$ . Lennard-Jones potential parameters  $\sigma/a = 0.8$ ,  $kT/\epsilon = 20$ .

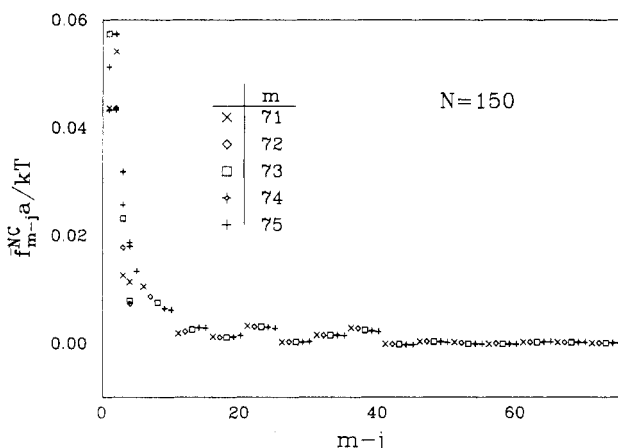


**Figure 8.** Spatial distribution of the transmitted noncovalent forces for different  $m$  as determined by molecular dynamics. The force  $\bar{f}_{m-j}^{NC}$  is the time-averaged noncovalent force exerted on atom  $j$  by atoms  $m + 1, \dots, N$ .  $r/Na = 0.1$ .

It may be shown<sup>2</sup> that for a sufficiently long-time average, the sum  $f_i$  should be constant along the entire length of the molecule, and this is seen to be the case within computational accuracy. The results in this figure, and in other calculations, show that the excluded volume or noncovalent forces  $f_i^{NC}$  are negative, corresponding to an internal pressure. For the zero axial force distance,  $r = r_0$ , these are just balanced by the covalent, tensile forces  $f_i^C$ .

The average spatial distribution of the noncovalent forces transmitted across an arbitrary bond was also determined. The force  $\bar{f}_{m-j}^{NC}$  is the time-averaged noncovalent force exerted on atom  $j$  by atoms  $m + 1, \dots, N$  so that

$$f_m^{NC} = \sum_{j=0}^m \bar{f}_{m-j}^{NC} \quad (17)$$

Typical values are shown in Figure 8; it is seen that  $\bar{f}_{m-j}^{NC}$  decays rapidly with  $m - j$  and is relatively independent of  $m$  for values of the latter index corresponding to the central portion of the chain.

## V. Effect of Chain-Chain Interaction

The work described in the previous two sections concerned excluded-volume effects on the force-length relation of a single long-chain molecule. In order to assess the effects of chain-chain interaction on this relation, we have also studied, by Monte Carlo simulation, the force-length

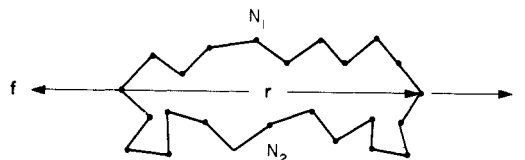


**Figure 9.** Pair of freely jointed chains with  $N_1$  and  $N_2$  bonds, respectively, and with common end points subject to prescribed displacement  $r$ ;  $f$  is time average of axial force required to maintain this displacement.

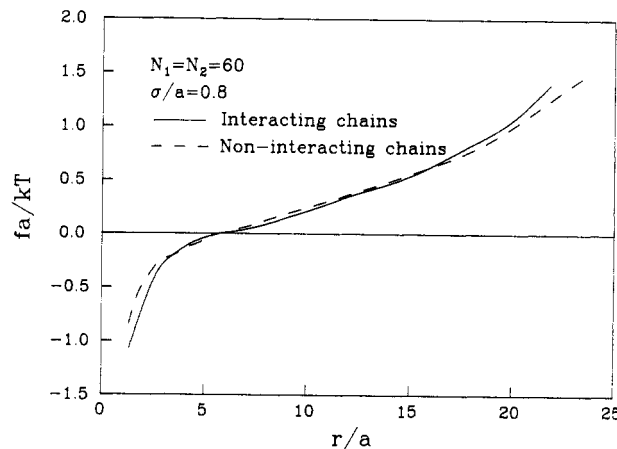


**Figure 10.** Force-length relation for pair of interacting chains with  $N_1 = N_2 = 60$  bonds compared with sum of forces in the same pair of noninteracting chains.

relation of two interacting chains with a common end-to-end displacement vector  $r$  (Figure 9). The chains have  $N_1$  and  $N_2$  bonds, respectively, and in addition to the covalent bonds connecting neighboring atoms, all of the atoms of the system interact with the hard-sphere potential of eq 2.

The model we are treating is seen to be equivalent to a single self-avoiding ring. This subject has been treated extensively<sup>19-21</sup> in the literature previously but, as with the linear chain, the work has focused on probability distributions and not on their implications for forces. In the absence of excluded volume, it follows readily from the result of Zimm and Stockmayer<sup>22</sup> that the force exerted by a chain pair is simply the sum of the forces exerted by the component chains. Here we explore this question in the presence of excluded volume.

The method of Monte Carlo simulation of this system is discussed in the Appendix. It is used to obtain the probability distributions  $P(r)$  and  $p(r)$ , and the force-length relation for the two interacting chains is obtained from the latter by use of eq 3.

Typical results for two interacting chains of equal length are shown in Figure 10. It is seen that the interaction between the two chains has only a secondary effect on the force-length relation for a single chain, and the force for the chain pair is very nearly twice that for a single chain.

Results for two interacting chains of unequal length are shown in Figure 11. It is seen that the assumption of additivity of the forces predicted by the force-length relations of the isolated chains provides a good approximation to the force observed in the interacting chains.

## VI. Conclusions

(1) As found previously for a chain with  $N = 10$  bonds, the force-length relation for the longer chains studied on the basis of the strain ensemble in this paper exhibits both compressive and tensile regions. However, while the relation for the short chain possessed a rather complex structure, due perhaps to the small value of  $N$ , the present

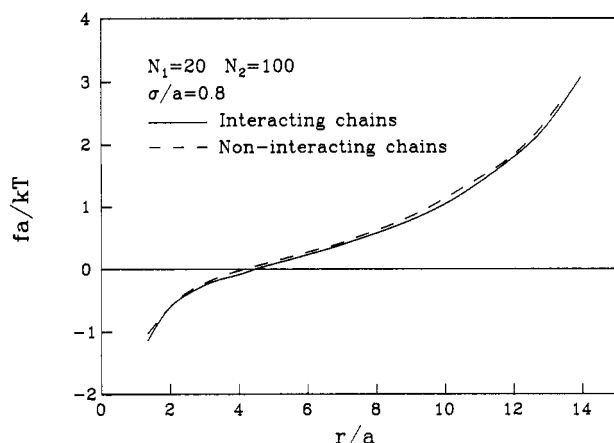


**Figure 11.** Force-length relation for pair of interacting chains with  $N_1 = 20$  bonds and  $N_2 = 100$  bonds, compared with sum of forces in the same pair of noninteracting chains.

results for large  $N$  are quite smooth and manifest all of the generally observed characteristics of experiments on rubber-like materials in uniaxial extension.

(2) The computed force-length relations for large  $N$  agree well in the compressive regime and for moderate extensions with those based on the probability distribution,  $p(\mathbf{r})$ , obtained by renormalization group methods by Oono et al.,<sup>15</sup> although the latter, as might be expected, does not show the force upturn at large extensions observed in the numerical results. The Monte Carlo results for chains with  $N = 200$  bonds also show a dependence on the hard-sphere diameter  $\sigma$ ; best agreement between the Monte Carlo and renormalization group results are obtained for  $\sigma/a = 0.4$ , where  $a$  is the bond length. Whether this  $\sigma$ -dependence persists for larger  $N$  remains a subject for future investigation.

(3) The fraction,  $E/D$ , of the volume in configuration space accessible to a phantom chain which is prohibited by excluded-volume interactions is quite large even at moderately large chain extensions and approaches unity rapidly as the chain length is decreased.

(4) Chain-chain interaction for a system of two chains has little effect on the force-length relation for a single chain.

(5) The molecular dynamics calculations of section IV provide physical insight into the nature of the noncovalent potential contribution to the forces in a long-chain molecule. They serve in several ways to confirm the results obtained through the numerical study of a different model in ref 2. In particular, the present calculations confirm the existence of a uniform central portion of the chain in which the noncovalent potential results in a decaying force or traction exerted across an arbitrary plane separating two portions of the chain.

(6) The usual three-chain model of rubber elasticity<sup>4</sup> does not explicitly consider excluded-volume effects; they are introduced implicitly through the phenomenological assumption that all deformations take place at constant volume. Although on the basis of purely entropic considerations the force-length relation of each chain is purely tensile, the behavior of the model in uniaxial extension exhibits both tensile and compressive regimes since it is assumed that excluded-volume effects produce the hydrostatic pressure required to satisfy the boundary condition of zero stress on the lateral faces. The present calculations show that the explicit consideration of excluded-volume effects in a strain-ensemble calculation of the force-length relation for a single chain leads to a relation that exhibits both compressive and tensile regimes

and the other generally observed characteristics of experiments on rubber-like materials in uniaxial extension.

## Appendix: Monte Carlo Procedure

To obtain the probability distribution function  $P(r)$  of the end-to-end distance for a single freely jointed chain with excluded volume, the "reptation" method<sup>23</sup> has been used. This algorithm samples configuration space in accordance with the probability density  $p(\mathbf{r})$ . Therefore it would require unattainable times to obtain sufficient points in the highly stretched  $r$  region. In order to obtain values of the function  $P(r)$  for large  $r$ , we replaced the usual transition probability<sup>24</sup>

$$W_{12} = \begin{cases} e^{(H(r_1)-H(r_2))/kT} & \text{if } H(r_2) > H(r_1) \\ 1 & \text{otherwise} \end{cases}$$

by

$$W_{12}' = W_{12}(f(r_2)/f(r_1))$$

where  $f(r)$  is chosen to be large for both small and large  $r$  in order to produce a more uniform sampling. The transition probability  $W_{12}'$  leads to a distribution  $p'(\mathbf{r}) = f(\mathbf{r})p(\mathbf{r})$ , from which the desired  $p(\mathbf{r})$  may be obtained. The choice of the bin size in  $r$  in which the configuration numbers are accumulated is based on two conflicting considerations. A smaller bin size permits greater accuracy in the computation of such quantities as  $r_0$ . On the other hand, a smaller bin size increases the fluctuations in the probability distribution and the subsequent errors in numerical differentiation. In our computations, the bin size was taken as  $0.1a$  to  $0.4a$ . The force-length curves obtained by numerical differentiation are then smoothed by a cubic spline method. The zero-force distance,  $r_0$ , is determined from these smoothed curves.

In the simulation of chain-chain interactions, the typical configuration is a chain loop with  $2N$  bonds. Choosing any pair of two atoms as the ends of two chains, we obtain a configuration for two chains with  $N_1$  and  $N_2$  bonds, with their ends tied together and with  $N_1 + N_2 = 2N$ . Therefore, from one configuration of the chain loop, we can determine many different configurations for two chains with preselected values of  $N_1$  and  $N_2$ .

The generation of such a chain loop as the initial configuration is done by a restricted random walk. We construct an  $N$ -step random walk with excluded volume on one side of a given plane with the start and end points on this plane. The other atoms are required to remain at a perpendicular distance from this plane which is greater than  $\sigma/2$ . Then the other half of the loop is obtained as the reflection of this  $N$ -bond chain about the plane.

To obtain a new configuration of the loop, a method that may be called a "shift and kink" move was employed. A given bond of the loop, bond  $i$ , with orientation vector  $\mathbf{d}_i$ , was chosen at random. The next  $N - 1$  bonds in the loop are moved by  $\mathbf{d}_i$  relative to the rest of the loop, so the vector  $\mathbf{d}_i$  becomes the bond at  $i + N$ . The Metropolis criterion is used to determine whether the new configuration is acceptable. Since this shift only rearranges the  $2N$  bonds of the loop, changing the relative angles between bonds, but not their orientations in space, it is supplemented periodically by a "kink-jump".<sup>25</sup> This causes a more uniform distribution in space of the individual bond orientations and helps to release some possible entanglements. If entanglements still occur, the computation is stopped and restarted from a new configuration. The other details are the same as in the single-chain case.

For  $N = 60$ , i.e., a loop with 120 bonds, 200 000 configurations were generated. The distribution function was found to remain stable from 100 000 iterations to 200 000

iterations. The CPU time required on the VAX 11/780 for such a computation was about 11 h and approximately 5 min on the Cray 1.

## References and Notes

- (1) This paper is based on the research of J. Gao performed in partial fulfillment of the requirements for the Ph.D. in Physics at Brown University. This work has been supported by the Gas Research Institute (Contract No. 5085-260-1152), by the National Science Foundation through the Materials Research Laboratory, Brown University, and by the National Science Foundation, Polymers Program, which provided computer time at the supercomputer center at the University of Minnesota.
- (2) Gao, J.; Weiner, J. H. *J. Chem. Phys.* **1984**, *81*, 6176.
- (3) Berman, D. H.; Weiner, J. H. *J. Chem. Phys.* **1985**, *83*, 1311.
- (4) Treloar, L. R. G. *The Physics of Rubber Elasticity*, 3rd ed.; Clarendon: Oxford, 1975; p 113.
- (5) Weiner, J. H. *Statistical Mechanics of Elasticity*; Wiley: New York, 1983.
- (6) See, for example: Munster, A. *Statistical Thermodynamics*, 1st English ed.; Springer: New York, 1969; Chapter IV.
- (7) Neumann, R. M. *Phys. Rev. A* **1985**, *31*, 3516.
- (8) Guyer, R. A.; Johnson, J. A. Y. *Phys. Rev. A* **1985**, *32*, 3661.
- (9) Weiner, J. H.; Berman, D. H. *J. Polym. Sci., Polym. Phys. Ed.* **1986**, *24*, 389.
- (10) Gō, N.; Scheraga, H. A. *Macromolecules* **1976**, *9*, 535.
- (11) Helfand, E. *J. Chem. Phys.* **1979**, *71*, 5000.
- (12) Pechukas, P. J. *J. Chem. Phys.* **1980**, *72*, 6320.
- (13) Weiner, J. H. *Macromolecules* **1982**, *15*, 542.
- (14) The numerical differentiation used the method of: Lanczos, C. *Applied Analysis*; Prentice-Hall: Englewood Cliffs, NJ, 1956; eq 5-8.4 with  $k = 5$  was employed with  $h = 0.1a$ .
- (15) Oono, Y.; Ohta, T.; Freed, K. F. *Macromolecules* **1981**, *14*, 880.
- (16) See also: Fleming, R. J. *J. Phys. A.: Math. Gen.* **1979**, *12*, 2157.
- (17) Reference 4, pp 232-233.
- (18) Flory, P. J. *Proc. R. Soc. London, Ser. A* **1976**, *351*, 351.
- (19) Lipkin, M.; Oono, Y.; Freed, K. F. *Macromolecules* **1981**, *14*, 1270.
- (20) Chen, Y. *J. Chem. Phys.* **1981**, *75*, 5160.
- (21) Baumgartner, A. *J. Chem. Phys.* **1982**, *76*, 4275.
- (22) Zimm, B. H.; Stockmayer, W. H. *J. Chem. Phys.* **1949**, *17*, 1301.
- (23) Webman, I.; Lebowitz, J. L.; Kalos, M. H. *Phys. Rev. A* **1981**, *23*, 316.
- (24) Binder, K., Ed.; *Monte Carlo Methods in Statistical Physics*; Springer-Verlag: Berlin, 1979.
- (25) Baumgartner, A. *J. Chem. Phys.* **1980**, *72*, 871.

## Tube Renewal in the Relaxation of 4-Arm-Star Polybutadienes in Linear Polybutadienes<sup>†</sup>

Jacques Roovers

Division of Chemistry, National Research Council of Canada, Ottawa, Ontario, Canada K1A 0R9. Received June 6, 1986

**ABSTRACT:** The terminal relaxation of a series of high molecular weight star polybutadienes ( $M$ ) dissolved at low concentration ( $c < 2.5\%$ ) in low molecular weight linear polybutadienes ( $P$ ) has been studied. The experimental conditions are favorable for the observation of relaxation by tube renewal of the stars. The longest relaxation time ( $\tau_1$ ) of stars with  $f = 4$  and  $f = 18$  can be superimposed on the values of  $\tau_1$  of linear polymers plotted against  $2M_w/f$ . It is found that  $\tau_1 \propto M_w^{2.2}P_w^{2.6}$ . The  $M^{2.2}$  dependence indicates that the tube around the test chain is a Rouse tube. The  $P_w^{2.6}$  dependence deviates considerably from the prediction of the reptation theory ( $P^3$ ). It is suggested that contour-length fluctuations are ineffective in tube renewal.

## Introduction

Reptation was originally devised as a model for diffusion and relaxation of linear polymers in the fixed surroundings of a network of entanglements.<sup>1</sup> Experiments that relate directly to this situation have been performed.<sup>2</sup> However, in linear polymer melts or concentrated solutions the entangling neighbors of a chain are not necessarily fixed on the time scale of the reptation of that chain. Neighboring chains reptate and abandon the entanglement. The imaginary tube around each polymer molecule is thereby locally and temporarily destroyed, and relaxation by lateral hopping becomes possible. This process is called tube renewal or constraint release.<sup>1</sup>

The relation between the primary reptation time  $\tau_{\text{rep}}$  and the longest tube renewal time  $\tau_R$  for a linear  $n$ -mer is given by<sup>3,4</sup>

$$\tau_{\text{rep}}(n) \propto \tau_0 n^3 / n_e \quad (1)$$

and

$$\tau_R(n) \propto N^2 \tau_{\text{rep}}(p) \quad (2)$$

where  $n$  and  $p$  are degrees of polymerization,  $n_e$  is the number of monomers between two consecutive entangle-

ments along the chain, and  $\tau_0$  is the time between jumps of the size of one monomer unit along the (curvilinear) tube. Equation 2 indicates that the relaxation by tube renewal is a Rouse type process, its longest time depending on the square of the number of entanglements per chain:  $N = n/n_e$ .<sup>1,5</sup> For homopolymer  $p = n$  and eq 2 becomes

$$\tau_R(n) \propto N^2 \tau_{\text{rep}}(n) \propto n^5 \quad (3)$$

The numerical coefficient in eq 2 and 3 has been estimated.<sup>3,5</sup> Tube renewal is expected to be less important than reptation for homopolymers. In the overall relaxation process other shorter Rouse relaxation times down to  $\tau_R(n)/N^2$  will also contribute, so that tube renewal modifies the longest relaxation time of a homopolymer.<sup>5,6</sup>

Tube renewal can be studied by observing the relaxation of an isolated long  $n$ -mer in a matrix of entangling low molecular weight  $p$ -mers.<sup>7</sup> It is required that no entanglements exist between the  $n$ -mers. Moreover, for a linear test chain, eq 1 and 2 require that  $nn_e^2/p^3 > 1$ , a condition that is not easily satisfied in practice.<sup>7</sup> Others have studied tube renewal in more concentrated mixtures of a large test chain in smaller chains.<sup>6,8</sup> Under these conditions both processes coexist, and there is a rather delicate interaction between tube renewal of  $n$ - $p$  entanglements and reptation along  $n$ - $n$  entanglements.<sup>6</sup>

The importance of tube renewal has been demonstrated very convincingly in the study of the diffusion of linear

<sup>†</sup> Issued as NRCC 26676.